UCRL-12056

UNIVERSITY OF CALIFORNIA
Lawrence Radiation Laboratory
Livermore, California

Contract No. W-7405-eng-48

MEASUREMENTS AT THE SOUTHERN MAGNETIC CONJUGATE REGION OF THE FISSION DEBRIS FROM THE STARFISH NUCLEAR DETONATION

Raymond G. D'Arcy
Stirling A. Colgate

September 11, 1964

Measurements at the Southern Magnetic Conjugate Region of the Fission Debris from the Starfish Nuclear Detonation

Raymond G. D'Arcy and Stirling A. Colgate

Lawrence Radiation Laboratory, University of California

Livermore, California

September 11, 1964

ABSTRACT

The fission products from the July 9, 1962, 'Starfish' high-altitude nuclear detonation have been measured with a recording gamma-ray spectrometer near the southern magnetic conjugate point of the Starfish location. The transit time of 2 to 20 sec over the 4000-km flight path indicates that debris arrived both noninteracted and interacted with the earth's atmosphere at the point of detonation. Since the southern magnetic conjugate point is below the horizon relative to the detonation point, all measured debris must have been ionized and guided by the geomagnetic field. The large fraction of debris observed (~ 50%) indicates the dominance of the geomagnetic field interaction. The spatial distribution of debris indicates that the major fraction arrived on the flux tube (~300 km width, flux surface L = 1.12) conjugate to the detonation point with a 2° westward drift. Additional debris was observed distributed southward up to L = 1.29 indicating a partial penetration across the flux surfaces of the geomagnetic field. The injection of high energy electrons into trapped orbits around the earth is identified with the beta decay in transit of the observed debris.

Using a recording gamma-ray spectrometer flown in a high altitude aircraft in the vicinity of the southern magnetic conjugate point of the July 9, 1962, Starfish high-altitude nuclear test we have measured a delayed gamma-ray flux from the fission product debris deposited at the top of the earth's atmosphere, presumably guided by the earth's magnetic field. We have measured the spatial distribution, time of arrival, and approximate absolute quantity of fission debris that interacted with the earth's magnetic field. Auroral effects from the Argus, Teak, and Orange tests [Matsushita, 1959; Newman, 1959; Cullington, 1958] indicated that an intense flux of beta particles was guided to the conjugate areas. However, the fission fragment debris deposition at a conjugate point had never been experimentally observed. The Argus tests, although detonated at approximately 500 km, a sufficiently high altitude for debris to escape the atmosphere, were too small in size (1 to 2 kilotons) for debris effects to be directly observable [Newman, 1959], and the Teak and Orange tests were so low in altitude (45 and 80 km) that the greater mass of swept-up neutral air would have maintained the debris neutral during expansion for a detonation of any yield [Colgate, 1963].

The Starfish nuclear test was carried out at 0900:09 UT on July 9, 1962, at an altitude of 400 km and with a yield of 1.4 megatons near Johnston Island [Brown, Hess and Van Allen, 1963]. At this altitude it is expected [Colgate, 1963] that a significant fraction of the debris will escape without interacting with the residual earth's atmosphere. The expansion of this debris will create a diamagnetic hole whose size is determined by the balance between magnetic pressure and the kinetic pressure of the expanding debris. A further extension of this picture would predict an expansion along the magnetic field with the debris plasma guided along a flux tube to its intersection with

the earth at the southern conjugate point. More detailed considerations [Colgate, 1963] would predict an unstable interaction of the plasma with the earth's field with a resulting mixing onto different flux surfaces. The distribution of debris trapped on various magnetic flux surfaces and the time spent in traversing the path on any particular flux surface to the southern conjugate point becomes important in calculating the injection of beta decay particles into trapped orbits in the geomagnetic field. Since only those beta particles with mirror points outside the earth's atmosphere will remain trapped, then only those beta decays occurring outside the earth's atmosphere can contribute directly to trapped radiation. Therefore the measurement of the location and arrival time of the fission debris at the southern conjugate point makes possible the calculation of beta injection into trapped orbits from the decay of this fission debris during its flight path of at least 4000 km from the detonation point to the southern conjugate region (see Figure 1).

PROCEDURE

An airborne gamma-ray spectrometer was used for this experiment. The detector consists of a cylindrical 3-in. × 3-in. NaI crystal, surrounded everywhere except at one end by a 3/8-in.-thick plastic anticoincidence scintillator cup for reducing charged-particle counting background. The detector was positioned horizontally with less than 1 g/cm^2 additional aircraft skin attenuation. The detector pulses are sorted by energy into 50 or 100 channels by a laboratory model pulse-height analyzer. In operation the spectrometer stores pulses for a preset interval, prints and punches out the spectrum and time on paper tape, clears itself, and automatically repeats the cycle (see Figure 2). This equipment was installed aboard a KC-135 aircraft operated by the Cambridge Air Force Research Center for upper

atmospheric radio propagation and radiation studies under the scientific direction of Dr. George Gassmann.

The flight pattern flown during the event is shown in Figure 3. The KC-135 attained an altitude of 43,000 ft (13 km) immediately before detonation time. The remainder of the flight path was flown at this altitude. The east-west pattern flown for 1 hour and 20 minutes after the detonation was intended to check on east-west debris motions either from upper atmospheric winds or continued deposition of trapped fission products. The lower energy limit of radiation accepted by the spectrometer was adjusted several times to the lowest value consistent with freedom from large dead time in the pulse height analyzer. The scale factor was also varied so as to cover the maximum energy range of the excess gamma radiation. Processing of the data was performed by computer, using the punched paper tape output of the spectrometer.

BACKGROUND

In the course of 20 flights with the same equipment in the North and South Pacific during the periods May 15 through July 12 and October 20 through November 3, 1962, the background gamma-ray spectrum from cosmic rays followed the altitude and latitude dependence of the soft component of cosmic rays. The background spectrum showed little structure, except for positron annihilation lines at 0.5 Mev and 1.0 Mev and slight contributions from debris contamination of the atmosphere at 0.75, 1.25, 1.60, and 1.95 Mev (see Figure 4). The background spectrum, uncorrected for detector efficiency, is seen to be rather steep at energies below 1.5 Mev and almost flat from 5 to 15 Mev (see Figure 5). The total flux of gamma rays ($\sim 5/cm^2$-sec) in this energy range, as well as the spectral shape, is in agreement with

several previous balloon measurements of the low-energy cosmic ray gamma-ray spectrum at similar altitudes [Anderson, 1961; Peterson, 1963; Vette, 1962]. At the altitudes (43,000-44,000 ft, or 13.0-13.3 km) and geomagnetic latitudes (12° S to 23° S) of interest in this study the background varied by approximately 5% per 1000 ft (300 m) in altitude and 1% per degree of latitude. During the period of this flight and all background flights, the constancy of the cosmic ray neutron monitor at Chicago (35° N) and at Huancayo (9° S) indicated a maximum change in cosmic ray gamma-ray background at these latitudes and at 43,000 ft of approximately 1% and so was neglected [Simpson, 1962; Ehmert et al., 1960]. Using the altitude and latitude corrections, we see in Figures 6 and 7 that the high energy part of the spectrum – well above the fission debris signal – agrees with the predicted background to within the statistical error.

CALIBRATION

The energy sensitivity of the gamma ray spectrometer varied with temperature over the 20-100° F ambient temperatures in the interior of the aircraft. Therefore in operation the spectrometer was calibrated periodically with Co^{60} and Cs^{137} gamma ray sources, in the 25-kev/channel mode of operation. Since all other energy ranges were selected by fixed resistor attenuation, these calibrations could then determine the energy sensitivity per channel in all modes of operation. In a typical background flight, the cabin temperature would drop suddenly by 30° F following the climb to 43,000 ft, after which the gain of the instrument would drop exponentially following the 15-min thermal time constant of the instrument. The slow temperature changes for the remainder of each flight would then permit a linear interpolation between gain calibrations (see Figure 8). During the Starfish

experiment, a calibration was made 2 min prior to the detonation. The gamma ray intensity from the Starfish event then remained so high that no further calibration was possible until 1 hr following the detonation. Therefore it is necessary to approximate the calibration drift over this interval by the previously observed exponential thermal drift between the measured end points. A maximum calibration error of up to 2% is thus possible 15 min after the detonation. The smaller drift between subsequent calibrations permitted an interpolation which is accurate within 1% (see Figure 8). With the steepest spectra observed both as background (see Figure 7) and as excess fission-product gamma rays (see Figures 4-7), a calibration error of 1-2% is equivalent to as much as 3-6% error in the low-energy gamma ray flux. Therefore, in the data processing no effort was made to quantize the calibration more accurately than half the known calibration error, or to adjust the background in more frequent steps than necessary to keep background errors below the known calibration error in the excess gamma-ray spectrum.

DECAY RATE CORRECTION

To obtain the overhead debris density as a function of aircraft location from the excess gamma-ray spectrum it is necessary to know the time dependence of both the gamma ray emission from fission products and the absorption of these gamma rays in the atmosphere (because of the decrease in average energy of gamma rays with increasing time after fission). The results of Zigman and Mackin [1961] have been used to plot the decay of gamma ray activity from 15 min to 5 hr after the detonation, in various energy groups of interest (see Figure 9). It may be seen that the time decay in the

energy group between 0.9 and 2.4 Mev may be closely approximated by the $t^{-1.2}$ rule, particularly in the period of greatest interest in this experiment, from 90 to 300 min after fission.

SPATIAL RESOLUTION

We assume that the debris is deposited in the earth's atmosphere at an altitude corresponding to its range at its mean velocity. For the measured transit time of $2 \pm 1/2$ seconds, this corresponds to 200 km stopping altitude so that the geometry becomes that of a plane source separated from a thin plane absorber immediately in front of a point detector. The local scale height $\left(\frac{1}{\rho}\frac{d\rho}{dt}\right)^{-1}$ of the earth's atmosphere at the detector is small, approximately 6 km, and corresponds to a thin absorber. In attempting to define the effective aperture of the detector we must consider both the direct and scattered photons. Fortunately, the steepness of the fission gamma spectra and the utilization of a spectrum cutoff above the Compton energy (mc^2) allows us to exclude the scattered photons from the observed signal. To demonstrate this we first define an effective aperture for nonscattered photons including attenuation as

$$\Omega = 2\pi \int_0^{\pi/2} \sin\theta \, e^{-n/\cos\theta} \, d\theta$$

where n is number of gamma-ray mean free paths of the residual atmosphere (160 g/cm^2). The maximum contribution occurs at an angle θ where at

10 Mev, n = 3.2: $\theta = 40°$, $\sin\theta = 0.64$

5 Mev, n = 4.6: $\theta = 35°$, $\sin\theta = 0.57$

1.5 Mev, n = 8: $\theta = 27°$, $\sin\theta = 0.45$

These effective apertures are large enough so that any photon scattered by

a mean angle $\sin\theta \approx 1/2$ suffers a fractional reduction in energy

$$\frac{h\nu'}{h\nu_0} = \left[1 + \frac{h\nu_0}{mc^2}(1-\cos\theta)\right]^{-1}$$

which is large enough so that its flux is small compared to the very much larger number of the same lower-energy photons present in the unscattered "steep" spectrum. As a consequence, the effective horizontal sensitivity of the detector for debris at altitude H is $\left(H\frac{\cos\theta}{\sin\theta}\right)$ giving approximately 100 km provided that a low-energy spectrum limit greater than 0.5 Mev is used. Figure 10 shows the integral gamma flux $0.75 \text{ Mev} \leq E \leq 2 \text{ Mev}$, as a function of time, distance, and earth's magnetic field lines (L value) [McIlwain, 1961], corrected for calibration, background, and fission decay rate. Structure with a half-width as small as 75 km is evident, which confirms experimentally a spatial resolution less than 100 km (see Figure 10).

It may also be seen that the same structure has a half-width of 120 km in the corrected excess gamma ray flux, $0.25 \leq E \leq 0.75$ (see Figure 11), confirming the presence of a higher fraction of scattered than unscattered gamma rays, and yielding a means of estimating the relative distance of discrete sources from the aircraft flight path from the relative amplitudes of the maximum corrected excess gamma ray fluxes in the two energy regions.

RESULTS - TIME

The initial rise of the gamma ray signal was faster than the data recording capability of the apparatus, but by using a stop watch the time of initial arrival was estimated at $2 \pm 1/2$ sec after the detonation. There was then a gradual further rise to a maximum at 20 sec after the detonation. The short time arrival corresponds to a transit velocity of 2×10^8 cm/sec, which

is the mean kinetic energy associated with a nominal megaton of energy in a nominal ton of matter [Colgate, 1963]. The large fraction of debris at a mean of 1/5 this velocity indicates a slowing-down mechanism which we interpret as interaction with the residual atmosphere in the neighborhood of the detonation.

RESULTS - SPATIAL, EARLY

The early intensity normalized according to $t^{-1.2}$, indicates a peak debris density at approximately 15° south latitude and 178° west longitude. This distribution is outlined in Figure 12 along with the exact conjugate point at 200 km altitude.

It may be noted from Figures 10 and 12 that the aircraft passed under a north-south maximum in debris density 5 min after the detonation and then began to turn east 8 min after the detonation, locating an east-west maximum at 10 min after the detonation, more than 200 km to the west of the true conjugate point. Four subsequent east-west passages verified a lack of major east-west motion of the debris due to high altitude winds. Therefore, it may be stated that the debris was initially deposited some 2° west of the true conjugate point to the detonation and that this displacement must have occurred in transit from the detonation rather than after deposition at the southern conjugate region.

An intensity peak in trapped radiation and atmospheric ionization at an L-value of 1.12 to 1.13 was measured over Johnston Island during the day following the detonation [O'Brien et al., 1962; Durney et al., 1962; Peiper, 1963; Rothwell et al., 1963], indicating the presence of a continuing debris maximum on these field lines, which passed 400 km over Johnston Island.

On the assumption of a mean 200-km stopping altitude for the fission debris in the southern conjugate region, which corresponds to the theoretical range of fission debris having the observed velocities, our observed early debris maximum corresponds to an L-value of 1.12 (see Figure 12) and is therefore most probably the strongest concentration of fission debris resulting from the detonation in the southern conjugate area [Colgate, 1963].

RESULTS - SPATIAL, LATE

Although no large east-west debris motion was observed in the 90 min following the detonation, there were indications of a slight southward motion of the early debris maximum. At later times (90 to 240 min after the detonation) a debris distribution with three distinct maxima was observed, the northmost maximum being 1-1/2° south of the maximum previously located at early times (see Figures 12, 13). The fine structure remaining in the debris distribution at these late times suggested a small collective southward motion of the debris with relatively little lateral diffusion. Therefore the northmost debris maximum observed at late times is probably the same as the single maximum observed at early times. It should be noted that the debris density observed at the southernmost point of the flight path, corresponding to a 200-km L-value of 1.29, is no more than 3% of the maximum in debris density earlier observed at an L-value of 1.12.

RESULTS - DEBRIS FRACTION

The initial time decay (300 sec) of the high energy portion of the spectrum (9-13 Mev) is shown in Figure 14 and compared to the $t^{-1.2}$ law. There is a marked difference between the expected fission decay and the observed decay. Also, the expected contribution from delayed fission gamma rays at these energies is negligible [Engle and Fisher, 1962; Maienschein et al., 1958].

Within minutes the energy spectrum steepens to the distribution expected from a fission spectrum at 43,000 ft (see Figure 6). A plot of the excess 9-13-Mev gamma rays fits a 22-sec and 55-sec decay component (see Figure 14) rather than a $t^{-1.2}$ decay. Thus, it is concluded that these are 10.8-Mev gamma rays from the $N_{14}(n,\gamma)$ capture [Groshev et al., 1959] of the thermalized 250-650-kev delayed neutrons emitted from Br^{87}, Br^{88}, and I^{137} decay products [Keepin et al., 1957; Perlow and Stehney, 1959] resulting from several fast decay chains in fission products. Preliminary computations on the basis of these 10.8-Mev neutron-capture gamma rays (see Appendix I) yield an estimate of 9×10^{10} fission products per square centimeter at Point A (see Figure 12). Integrating over the measured debris distribution (Figure 13) results in 45% of the total debris in the southern conjugate area covered by the flight, assuming one megaton of U^{235} fission products and a symmetrical east-west debris distribution as measured near the point of maximum debris density. Taking into account more accurate yield of Br^{87}, Br^{88}, and I^{137} should not change this estimate more than a factor of 2. The attenuation of gamma rays produced by neutron capture at various depths in the atmosphere is a greater source of inaccuracy, although subject to a more rigorous calculation.

INTERPRETATION

1. Since neutral debris could not have reached the southern conjugate area from the Starfish detonation (see Figure 1), this measurement of a major fraction of the Starfish debris in a restricted area indicates that the initial dynamics of the mass motion of the Starfish debris were largely controlled by the interaction of an ionized expanding debris plasma with the geomagnetic field. As already pointed out, the prompt arrival of a small

debris fraction indicated the direct escape of this fraction along the lines of the geomagnetic field at a velocity of 2×10^8 cm/sec. However, the relatively late arrival of a large fraction indicates that it must have interacted cooperatively with approximately 20 times its own mass of air (assuming energy conservation) in order to result in the observed mean reduced velocity of 4×10^7 cm/sec. The concept of depositing the detonation energy in a cubic scale height of the atmosphere predicts [Colgate, 1963, Eq. (20)] a slowed-down debris velocity $U_{ex} \approx 4 \times 10^7$ cm/sec for an atmospheric particle density of $n_0 = 10^8$/cc at 400 km. The most optimistic collisional interaction (the free-electron dynamic friction) requires 100 times this density to stop the debris within a distance of a scale height (70 km) and so we are led to consider cooperative phenomena to explain the observed interaction. The time-dependent ionization of the neutral air within the combined moving debris plasma and magnetic field (neutral stress magnetic shock) is consistent with the observations. The magnitude of the total deposited debris fraction (~50%) further emphasizes the cooperative interaction with the geomagnetic field.

2. The distribution of debris in space (Figure 1) indicates that the combined debris-air plasma was not confined to a flux tube determined solely by diamagnetic forces, but instead reached geomagnetic flux surfaces $L \approx 1.3$ significantly greater than the detonation point $L = 1.12$. The distribution of debris as a function of L-value is most likely a measure of the Taylor-like plasma magnetic field instability, but the possibility of debris crossing to higher flux surfaces in the neutral state cannot be ruled out experimentally. However, theory [Colgate, 1963] would indicate that the electron temperature should be high enough, $T_e \approx 18$ ev, so that the probability of the neutral state should be extremely small.

3. The observed 220-km westward drift of the debris maximum from the simultaneously measured conjugate point [Leonard, 1963] is more than two and one-half times the drift expected for singly charged debris ions with the observed velocity of 2×10^8 cm/sec and a mean atomic number of 100, using the guiding center approximation and the methods of Hamlin et al. [1961] and Lew [1961]. However, we note from Figure 13 that the initial interaction of the debris with the geomagnetic field must have been as a plasma, to produce the several distinct debris maxima. Consequently, it should not be expected that single-particle orbit theory can be relied upon to predict the drift in longitude during the initial trajectory of the debris.

4. The inclination of the magnetic field lines near the largest debris maximum corresponds to 1-1/4 to 1-1/2° southward shift per 100 km drop in altitude for the debris. The experimental results indicate a southward motion of 1-1/2° from 5 min to 150 min after the detonation, with very small lateral diffusion, because of the preserved fine structure. This is consistent with the picture that the debris fell about 100 km from the stopping altitude of above 200 km in an ionized state and therefore was constrained to move southward along magnetic field lines. The ionized state is preserved because the incident debris kinetic energy as well as beta decay energy is sufficient to maintain an ambient temperature of several electron volts for several minutes. It should be noted that the 200-km L-values used in Figures 9-13 are chosen only to represent a mean debris altitude somewhere between the expected initial stopping altitude of somewhat above 200 km [Colgate, 1963] and the lower altitudes in the vicinity of 150 km to which the debris would be expected to fall many minutes after the detonation. Although it is expected that the L-value traversed by the debris from the detonation to the southern conjugate

region will be within 0.02 of the L-values indicated in Figures 9-13, any more accurate L-value requires more accurate knowledge of the altitude of the debris as a function of time and the wind motion of the debris than could be measured by this experiment alone.

5. Since the injection of trapped electrons into the geomagnetic field requires that the point of origin of the electron be within the confinement volume (virial theorem), then beta decay of fission debris in the earth's atmosphere cannot contribute to injection, except by an unlikely favorable scatter of such electrons out of the loss cone, while in the containment volume. Therefore only that fission debris beta-decaying in transit through the trapping volume can contribute strongly to injection, so that the debris observed at the southern conjugate point (and only this debris) should have injected most trapped electrons during transit, rather than thereafter. Since this transit time is only weakly dependent upon L-value, we expect the distribution of observed deposited debris to be a fair approximation to the trapped beta injection. However, it should be pointed out that more than two-thirds of the debris measured in this experiment was located on magnetic shells below $L = 1.18$ (see Figure 10), where the lifetime for trapped beta-decay electrons is at most a few hours. Therefore, the detailed structure of the two highest debris maxima could not have been observable in the trapped radiation. Since the debris transit occurred early in time, the resulting trapped electrons correspond to relatively high energy betas. The measured presence of a relatively large soft component at large L-values [Brown and Gabbe, 1963; West et al., 1964] is not explained by either the present measurements or model and must await further considerations most probably of collision-free shocks or late neutral debris injection.

APPENDIX I

We expect a small fraction of the fission debris decay chain to emit delayed neutron groups. The two delayed neutron groups observable after 50 sec are as follows [Keepin et al., 1957; Perlow and Stehney, 1959]:

Precursor isotope	Time constant (sec)	Neutron energy (kev)	Fraction n/fission (%)
Br^{87}	55	250	0.063
I^{137}, Br^{88}	22	450	0.35

Approximately half of these neutrons will escape into space, and half will thermalize in the atmosphere, to be absorbed largely by the processes $N^{14}(n,p)\,C^{14}$ and $N^{14}(n,\gamma)$ with thermal cross sections 1.76 [Colmer and Littler, 1950] and 0.08 barns [Groshev et al., 1959], respectively. Also 11% of these $N^{14}(n,\gamma)$ captures will result in an isotropically emitted 10.8-Mev gamma ray [Groshev et al., 1959]. Therefore, the flux of 10.8-Mev gamma rays near the top of the atmosphere is a fraction 0.0055 of the incident downward flux of neutrons. Since the absorption length of 10.8-Mev gamma rays in air is 50 g/cm^2 and the measurement was taken at an atmospheric depth of 165 g/cm^2 (43,000 feet), to a first approximation both the forward Compton scattering of the gamma rays and the depth dependence of the neutron thermalization may be neglected. The effective area of our detector for 10.8-Mev gamma-ray absorption is 9 cm^2 [Miller and Snow, 1960, 1961]. The measured flux at 50 sec is thus 3.5/cm^2-sec, 1.0/cm^2-sec of which is attributable to the Br^{87} component:

$$\psi_\gamma = (1 - R)fEE'\Omega\, e^{-NX}\, \frac{1}{\tau}\, e^{-tK}$$

R = albedo (0.67)

f = delayed neutron fraction (6×10^{-4})

E = capture probability to γ-emitting state (5%)

E' = probability of 10.8-Mev γ/capture (11%)

τ = decay time (54.5 sec)

NX = 2-1/3 mean free paths (average path from neutron thermalization and capture)

$\Omega = \frac{0.4}{4\pi} = 0.032$ = angular factor for 10.8-Mev γ's

Hence

$$\psi_\gamma = 5.6 \times 10^{-11}\ e^{-t/55}\ \gamma\text{'s/fission-cm}^2\text{-sec from the Br}^{87}\text{ fraction.}$$

An approximate integration over the limits of the time-corrected contours shown in Figure 13, assuming a symmetrical east-west distribution, yields an effective area of 1.5×10^5 km^2 for the maximum debris density measured at point A. Assuming a total of 1 megaton of U^{235} fast fission products from the explosion, assuming 1.5×10^{26} fissions per megaton, and taking F as the fraction of total fission products spread over the effective area at point A, we have 10^{11} F fissions/cm^2, or a 10.8-Mev gamma-ray flux of 5.6 $Fe^{-t/55}$ photons/cm^2-sec. This gives F = 0.45 for a preliminary estimate of the fraction of the debris in the southern conjugate area.

Acknowledgments. We should like to thank the personnel of DASA Project 6.10 for their assistance in this experiment; in particular credit is due to the Aircraft Commander, Major R. Creager, and to Captain K. Crookes, who piloted the KC-135 aircraft under extreme conditions of altitude and endurance, to Captain E. Carr and Lieutenant F. Fisher, who navigated a rapidly changing flight plan with great accuracy, to J. Gauger and T. Barrett, for their cooperation and assistance in carrying out the experiment, and to G. Gassmann for his support of this experiment and his planning of the flight path for the best combination of radiation and radio propagation measurements.

We are also indebted to O. Barlow, R. Swenson, and R. Blenz for the design, construction, and maintenance of the equipment, to Major R. Dowd and R. Whidden for their assistance with the installation of the equipment in the aircraft and with logistical support in the field, and to B. Gumm, G. Lentz, L. Littleton, A. Lukey, J. McCall, and E. Myles for the computer processing of the data. We have benefited from discussions of the results with J. Carpenter, T. Stinchcom, and E. Stone.

We should also like to thank J. A. Simpson for his continued support and encouragement of this experiment, and for his advice throughout.

The aircraft was operated by the Upper Atmosphere Physics Laboratories of the Air Force Cambridge Research Laboratories, Bedford, Massachusetts, U. S. Air Force Office of Aerospace Research.

One of the authors (Raymond G. D'Arcy) was at the Enrico Fermi Institute of Nuclear Studies of the University of Chicago, during the performance of this experiment, and during a large part of the data analysis.

This research was supported in part by the U. S. Air Force Geophysics Research Directorate under Contract No. AF 19(604)-4554, the National Aeronautics and Space Administration under Grant No. NsG 179-61, and the U. S. Atomic Energy Commission.

REFERENCES

Anderson, K. A., Cosmic ray photons below cascade energy, Phys. Rev., 123, 1435-1439, 1961.

Brown, W. L., and J. D. Gabbe, The electron distribution in the earth's radiation belts during July 1962 as measured by Telstar, J. Geophys. Res., 68, 607-618, 1963.

Brown, W. L., W. N. Hess, and J. A. VanAllen, Introduction, collected papers on the artificial radiation belt from the July 9, 1962, nuclear detonation, J. Geophys. Res., 68, 605-606, 1963.

Colgate, Stirling A., The phenomenology of the mass motion of a high altitude nuclear explosion, UCRL-7224, Rev. II, 1963.

Colmer, F. C. W., and O. J. Littler, Pile neutron absorption cross sections, Proc. Phys. Soc. (London), A63, 1175, 1950.

Cullington, A. L., A Man-made or artificial aurora, Nature, 182, 1365-1366, 1958.

Durney, A. C., H. Elliot, R. J. Hynds, and J. J. Quenby, Satellite observations of the energetic particle flux produced by the high altitude nuclear explosion of July 9, 1962, Nature, 195, 1245-1248, 1962.

Ehmert, A., H. Erbe, G. Pfotzer, C. D. Anger, and R. R. Brown, Observations of solar flare radiation and modulation effects at baloon altitudes, July 1959, J. Geophys. Res., 65, 2685-2694, 1960.

Engle, L. P., and P. C. Fisher, Energy and time dependence of delayed gammas from fission, LAMS-2642, 1962.

Groshev, et al., Atlas of γ-Ray Spectra from Radiative Capture of Thermal Neutrons, Pergamon Press, New York, 1959.

Hamlin, D. A., R. Karplus, R. C. Vik, and K. M. Watson, Mirror and azimuthal drift frequencies for geomagnetically trapped particles, J. Geophys. Res., 66, 1-4, 1961.

Harrison, Robert E., Kenneth W. Hubbard, Fred L. Keller, and James I. Vette, Plots of constant B and constant L for various longitudes, SSD-TDR-63-221, 1963.

Keepin, G. R., T. F. Wimett, and R. K. Zeigler, Delayed neutrons from fissionable isotopes of uranium, plutonium, and thorium, Phys. Rev., 107, 1044-1049, 1957.

Leonard, Robert S., Selection of a model of the earth's magnetic field, J. Geophys. Res., 68, 6437-6440, 1963.

Lew, John G., Drift rate in a dipole field, J. Geophys. Res., 66, 2681-2685, 1961.

Matsushita, Sadami, On artificial geomagnetic and ionospheric storms associated with high altitude explosions, J. Geophys. Res., 64, 1149-1161, 1959.

Maienschein, F. C., R. W. Peelle, W. Zobel, and T. A. Love, Gamma rays associated with (thermal U^{235}) fission, in Proceedings of the Second United Nations International Conference on the Peaceful Uses of Atomic Energy, 15, p. 366ff., 1958.

McIlwain, Carl E., Coordinates for mapping the distribution of magnetically trapped particles, J. Geophys. Res., 66, 3681-3891, 1961.

Miller, W. F., and W. T. Snow, Energy loss spectra in NaI, Rev. Sci. Instr., 31, 39, 1960; expanded in ANL-6318, 1961.

Newman, Phillip, Optical, electromagnetic and satellite observations of high-altitude nuclear detonations, part I, J. Geophys. Res., 64, 923-932, 1959.

O'Brien, B. J., C. D. Laughlin, and J. A. Van Allen, The geomagnetically trapped radiation produced by a high altitude nuclear explosion on July 9, 1962, Nature, 195, 939-943, 1962.

Peiper, G. F., A second radiation belt from the July 9, 1962, nuclear detonation, J. Geophys. Res., 68, 651-655, 1963.

Perlow, Gilbert J., and Andrew F. Stehney, Halogen delayed neutron activities, Phys. Rev., 113, 1269-1276, 1959.

Peterson, Laurence E., The 0.5 Mev gamma ray and the low energy gamma ray spectrum to 6 grams per square centimeter over Minneapolis, J. Geophys. Res., 68, 979-987, 1963.

Rothwell, P., J. H. Wagner, and J. Sayers, Effect of the Johnston Island high altitude nuclear explosion on the ionization density in the topside ionosphere, J. Geophys. Res., 68, 947-949, 1963.

Simpson, J. A., private communication, 1962.

Vette, J. I., Low energy gamma rays produced in air and lead by cosmic rays, J. Geophys. Res., 67, 1731-1739, 1962.

West, H. I., Jr., L. G. Mann, and S. O. Bloom, Some electron spectra in the radiation belts in the fall of 1962, UCRL-7659; Proc. Fifth Intern. Space Science Symposium, North-Holland, Amsterdam, 1964.

Zigman, P., and J. Mackin, Gamma energy release and ionization rates following thermal neutron fission of U^{235}, Health Phys, 5, 79-85, 1961.

/no

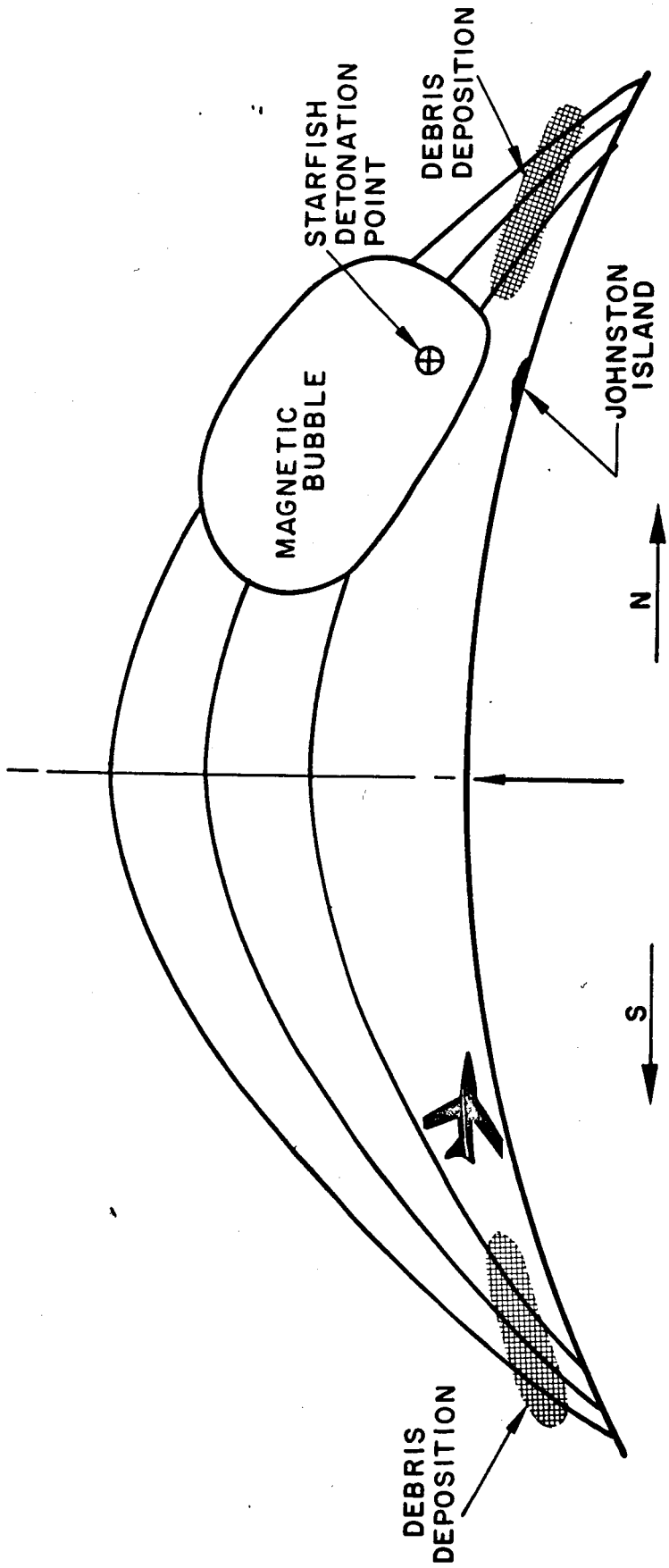

Fig. 1. Geometry of debris motion from detonation to southern conjugate region. (Field lines approximate.)

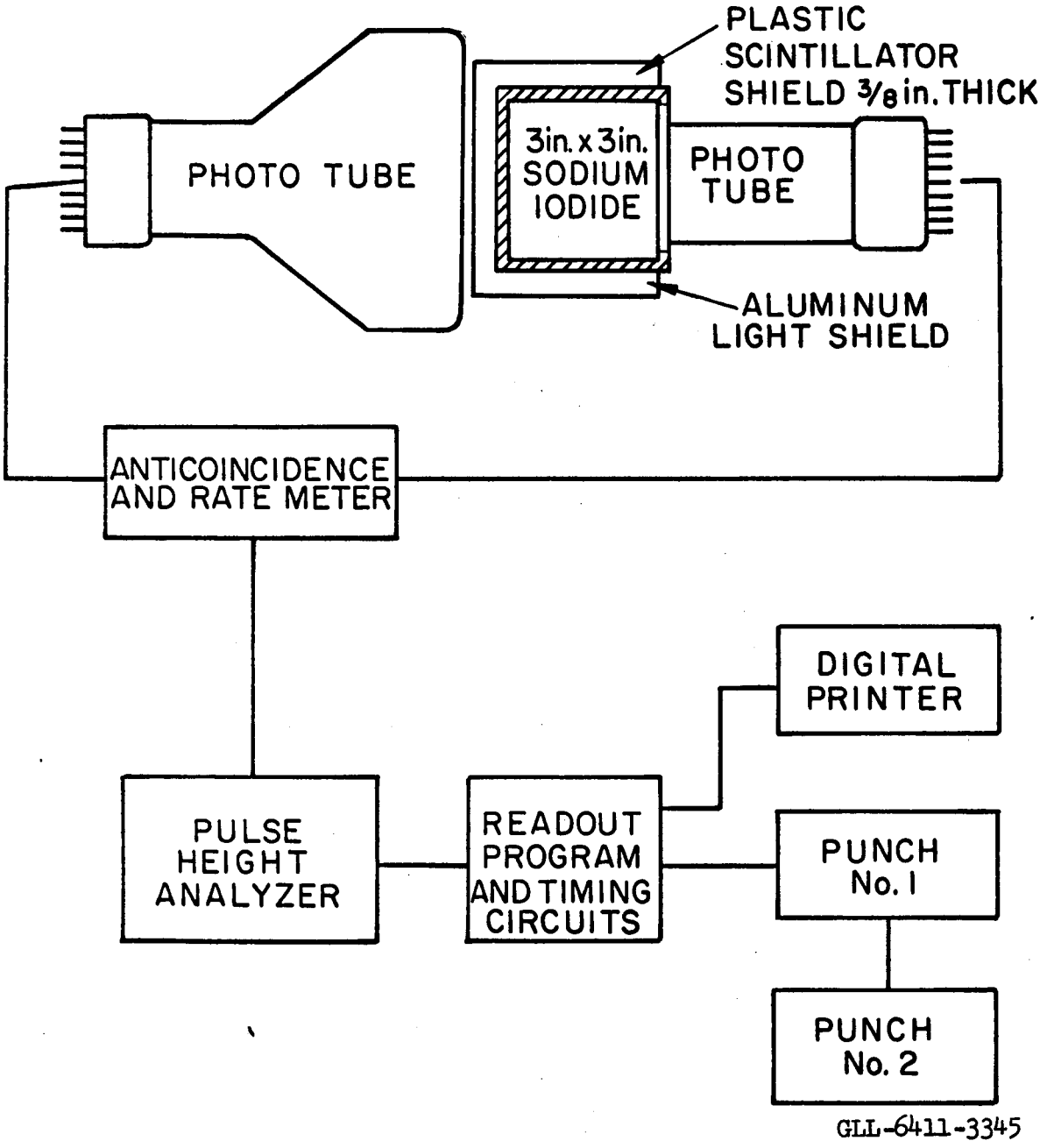

Fig. 2. Block diagram of gamma ray spectrometer.

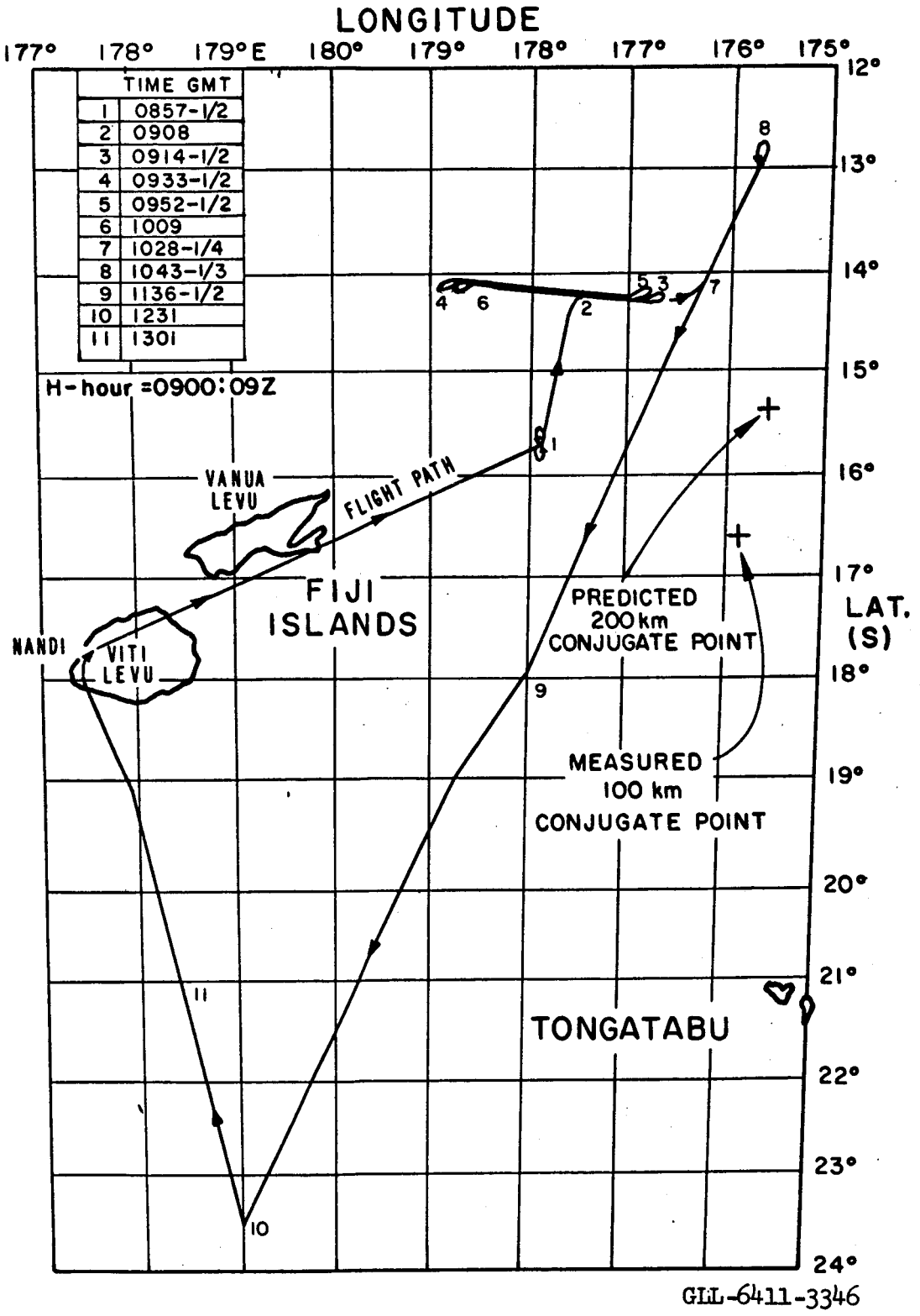

Fig. 3. Flight path of aircraft following the detonation, showing measured conjugate point to detonation at 100 km and calculated conjugate point at 200 km [Leonard, 1963].

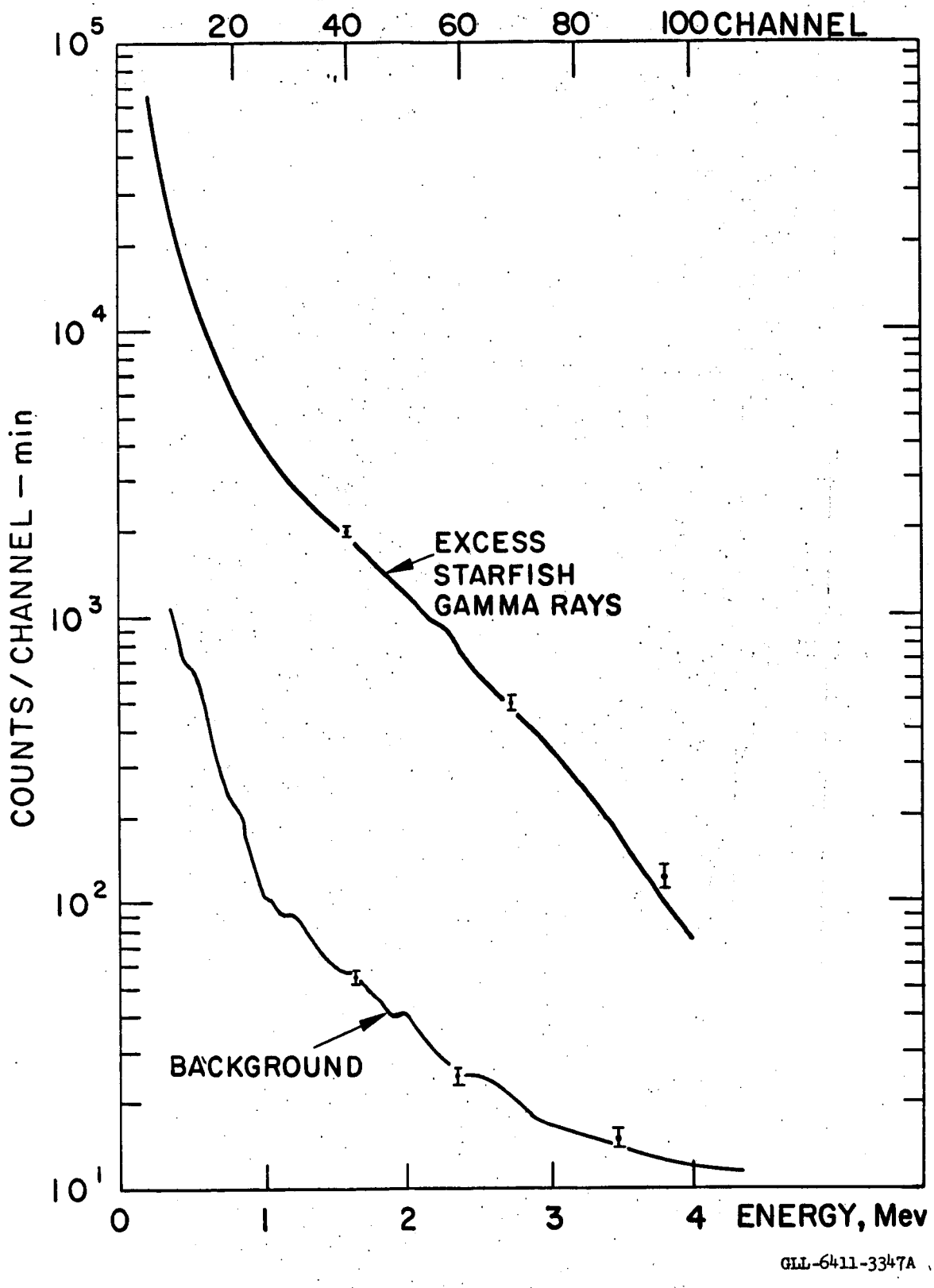

Fig. 4. Excess gamma-ray spectrum 30 min after detonation, together with background.

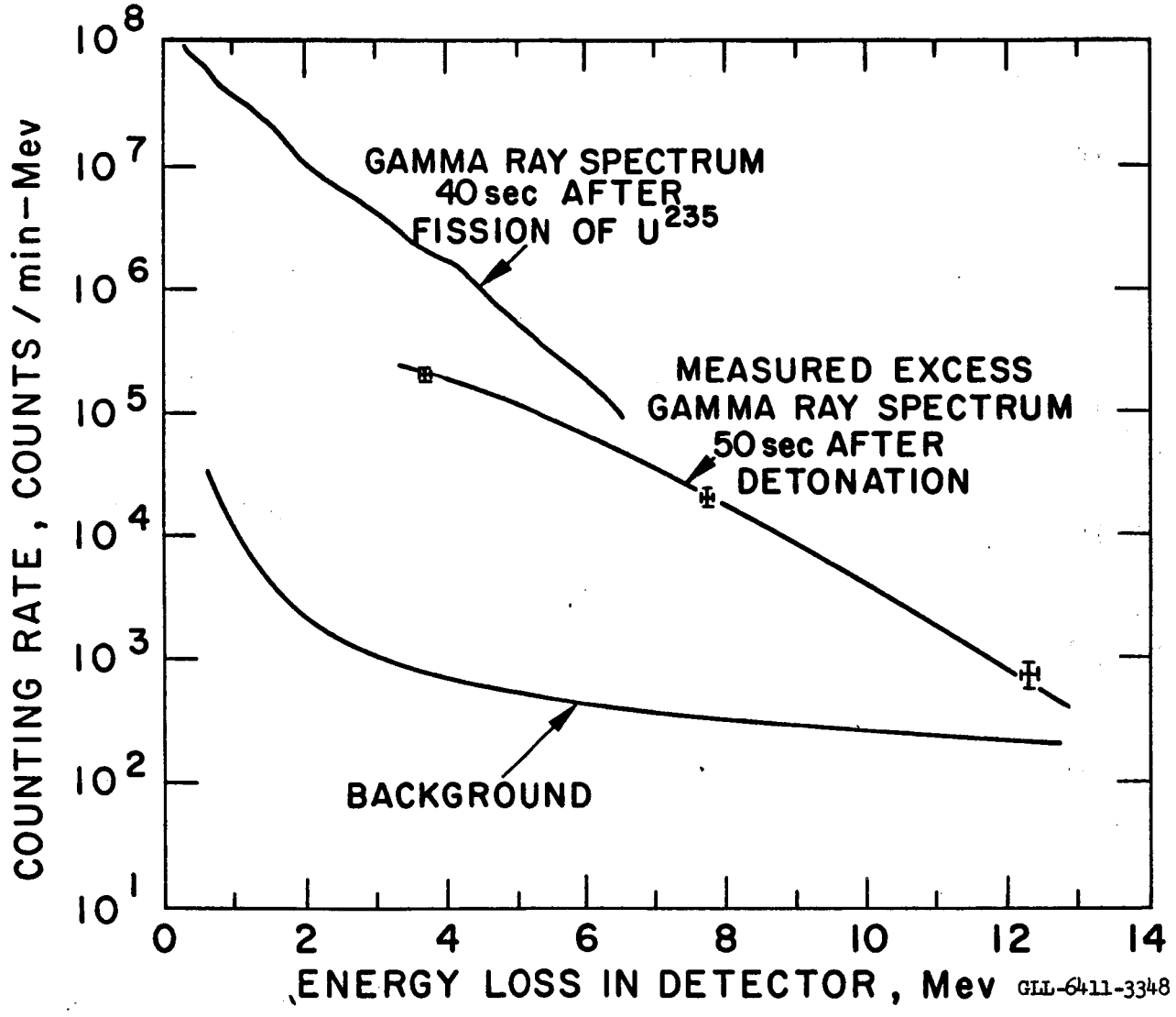

Fig. 5. Excess gamma-ray spectrum 50 sec after detonation, together with expected fission spectrum and background [Engle and Fisher, 1962].

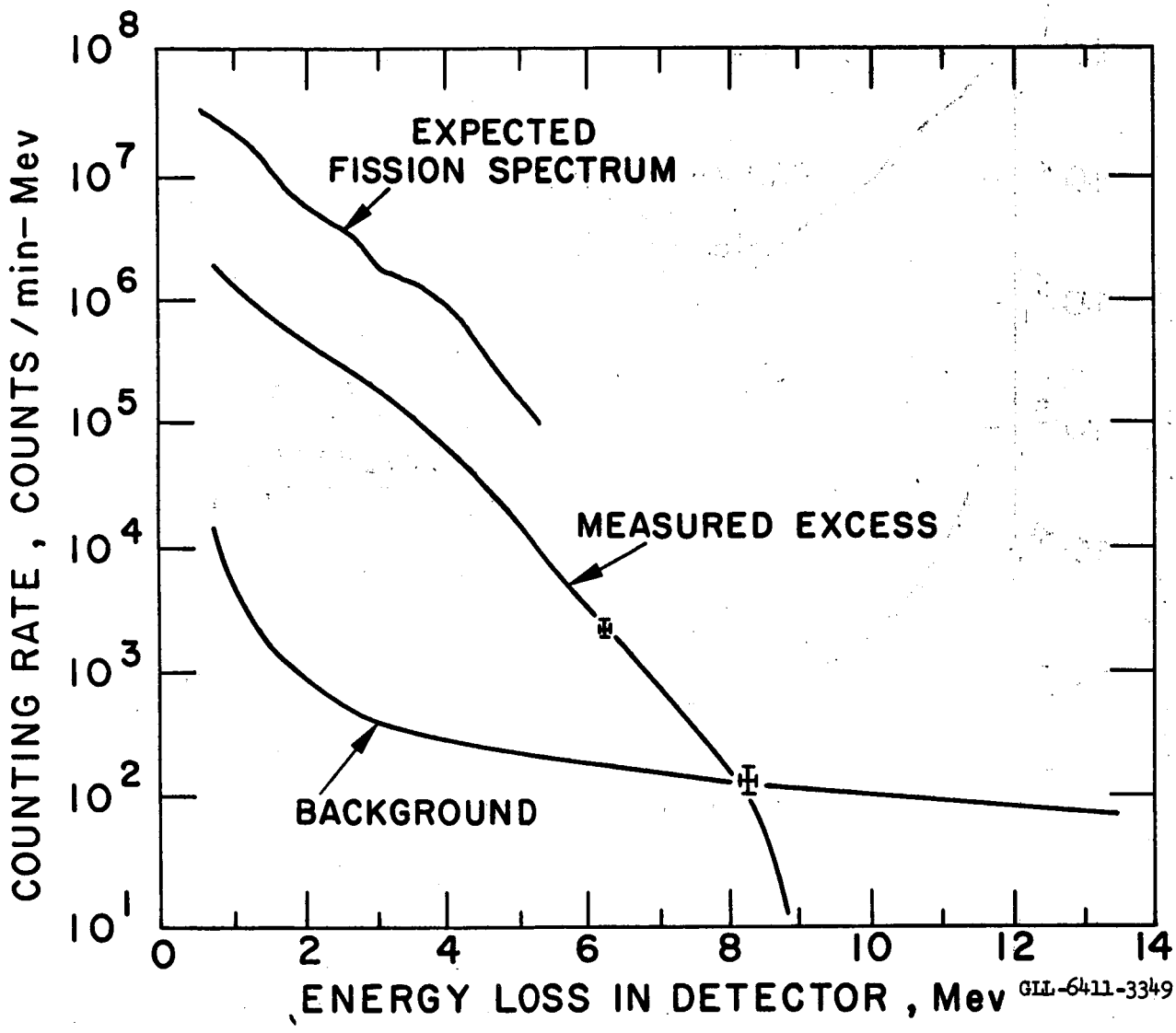

Fig. 6. Excess gamma-ray spectrum 5 min after detonation, together with background and expected fission spectrum [Zigman and Mackin, 1961].

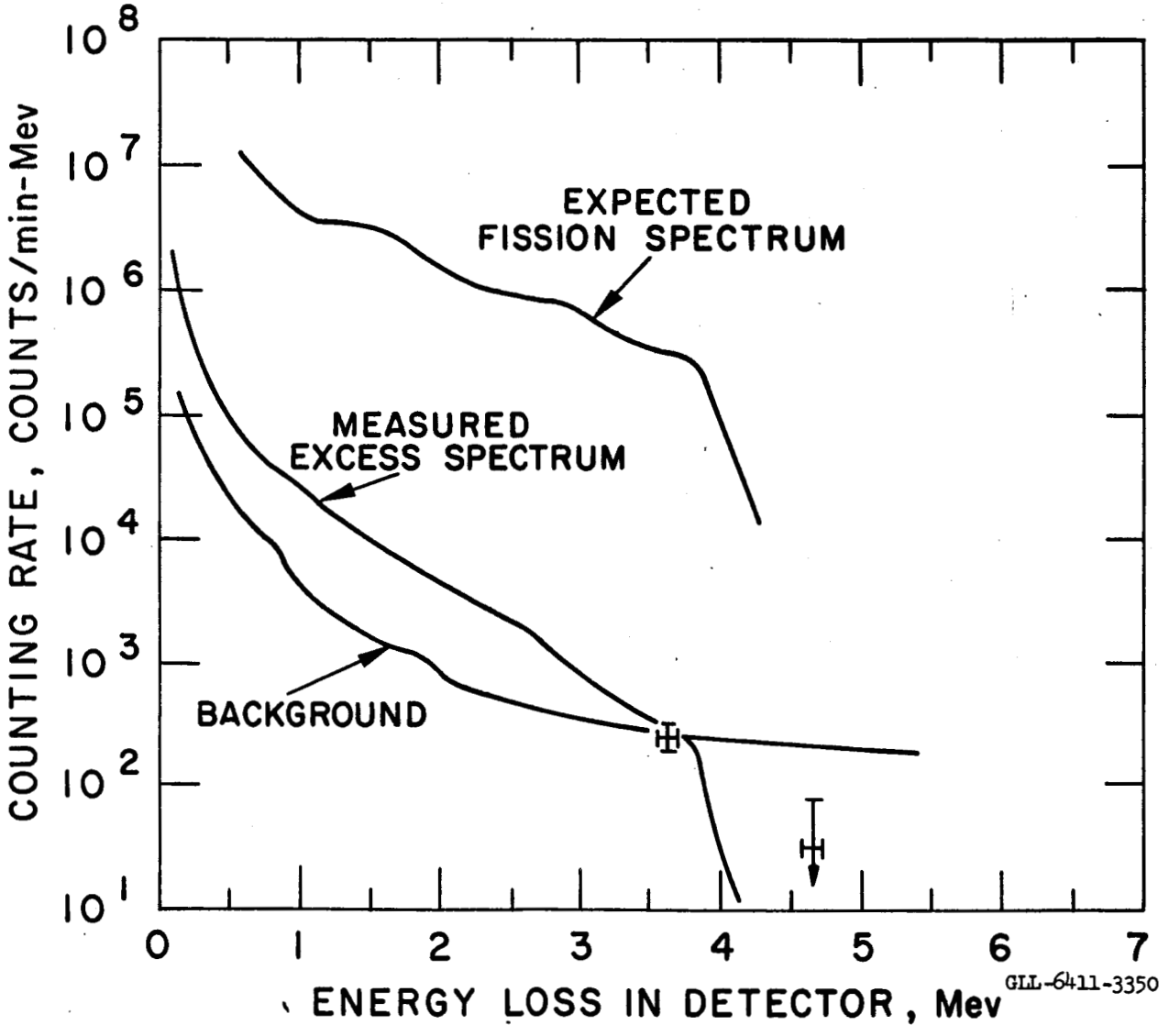

Fig. 7. Excess gamma-ray spectrum 150 min after detonation, together with background and expected fission spectrum [Zigman and Mackin, 1961].

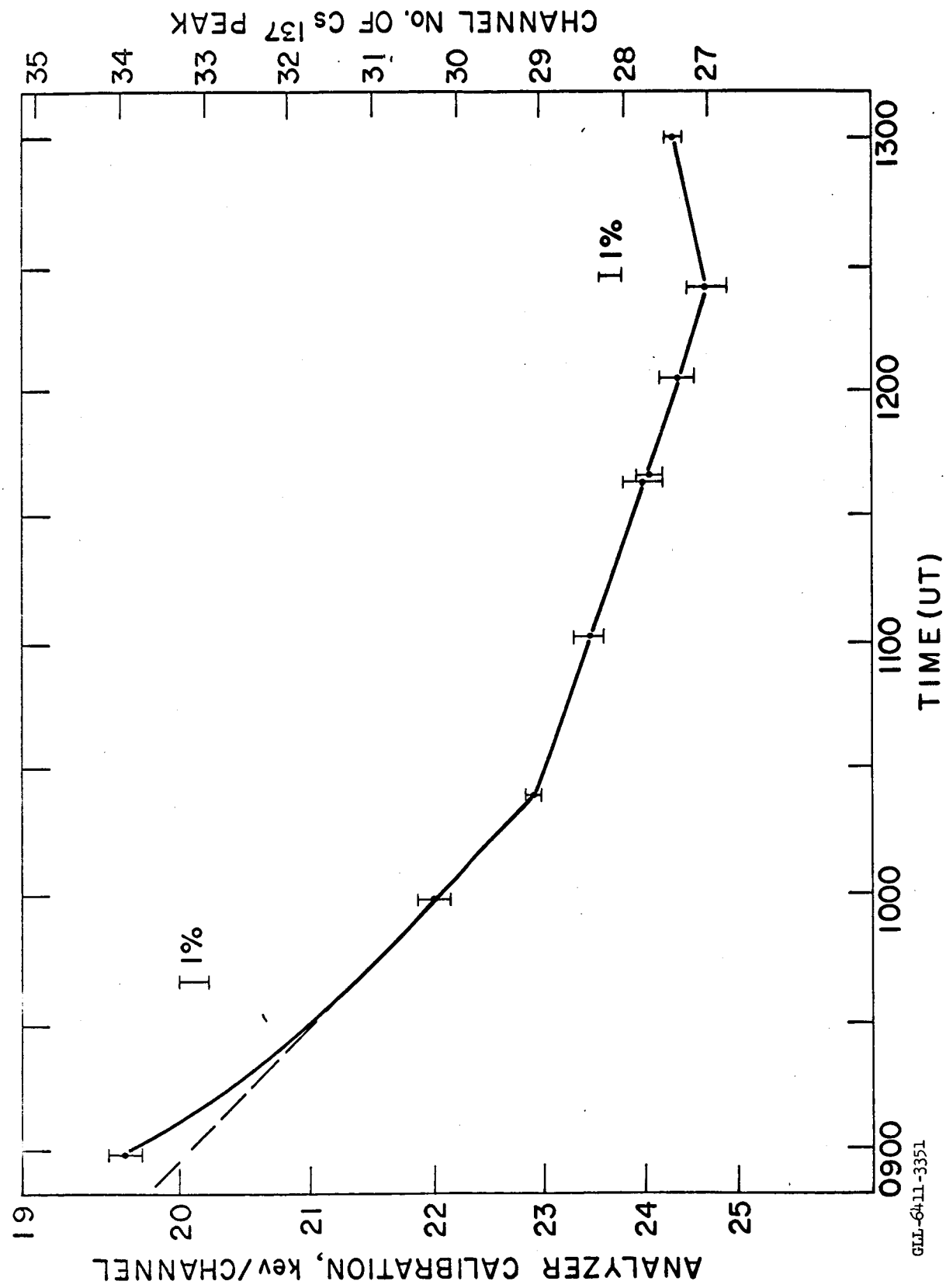

Fig. 8. Energy calibration of spectrometer during Starfish measurements.

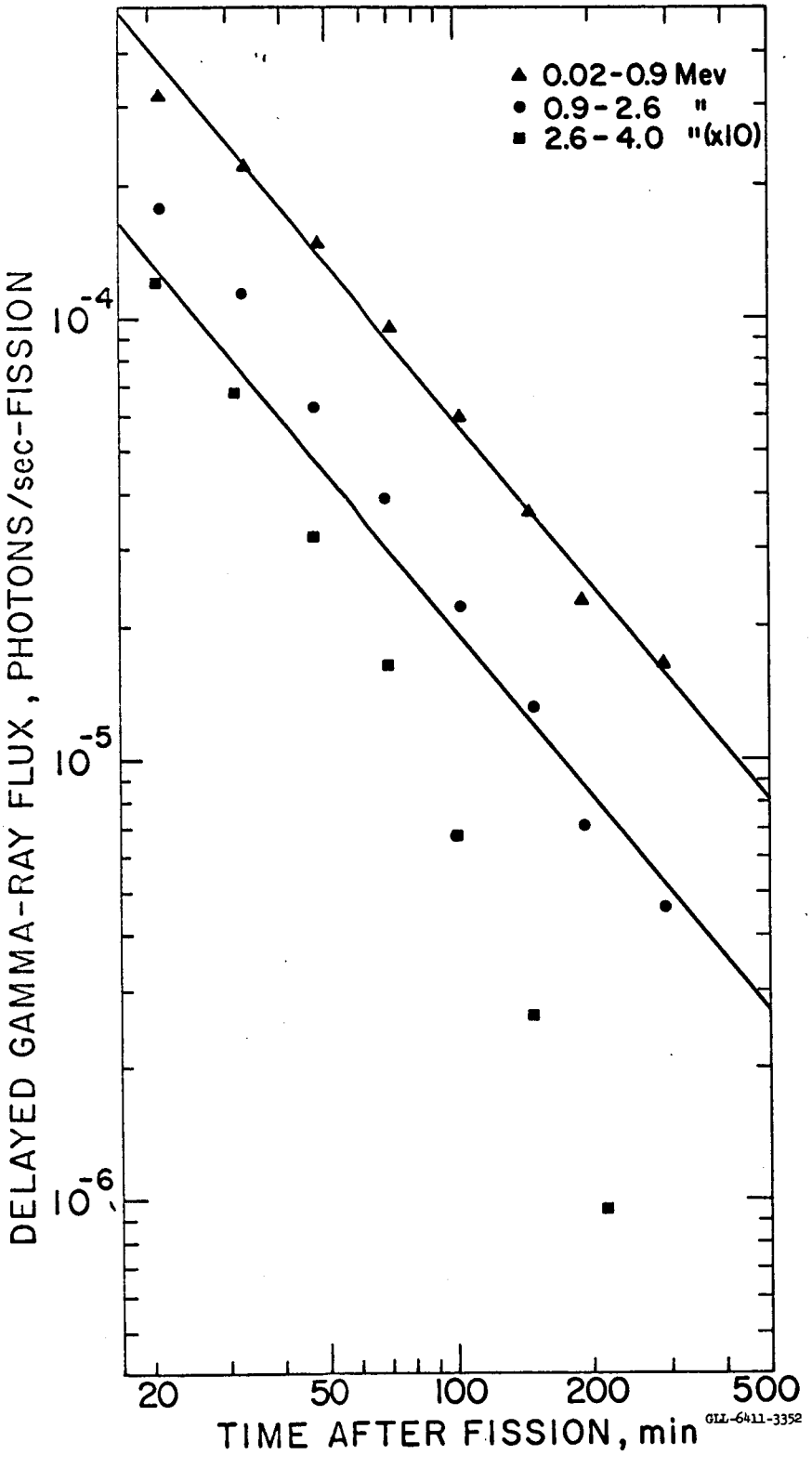

Fig. 9. A comparison of the time decay of delayed gamma rays from U^{235} fission in three energy groups with $t^{-1.2}$ decay [Zigman and Mackin, 1961].

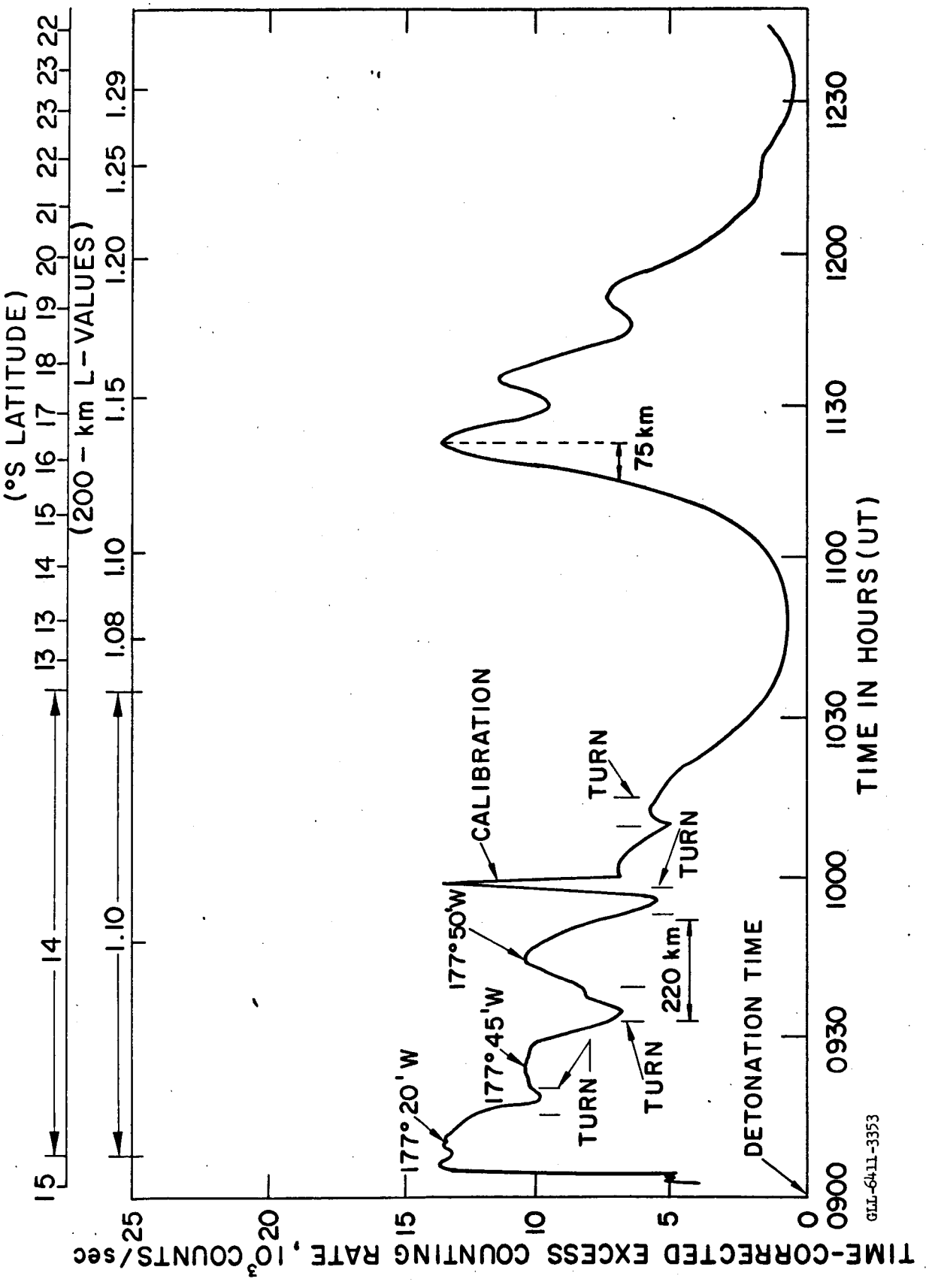

Fig. 10. Excess gamma rays between 0.75 and 2.0 Mev, normalized to 10,000 sec after the detonation by the $t^{-1.2}$ law. Variations during turns of the aircraft reflect the strong north-south gradient.

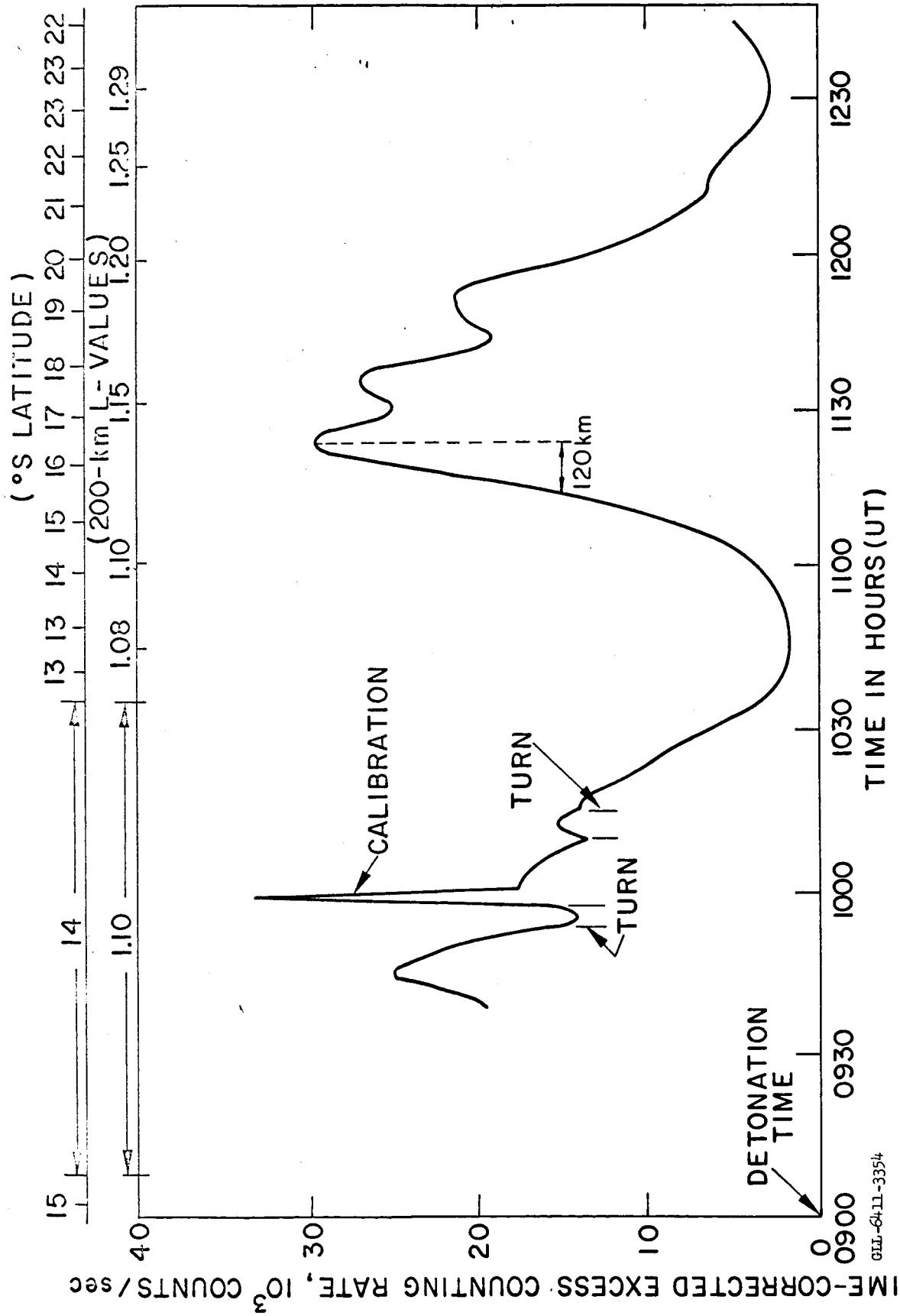

Fig. 11. Excess gamma rays between 0.25 and 0.75 Mev, normalized to 10,000 sec after the detonation by the $t^{-1.2}$ law.

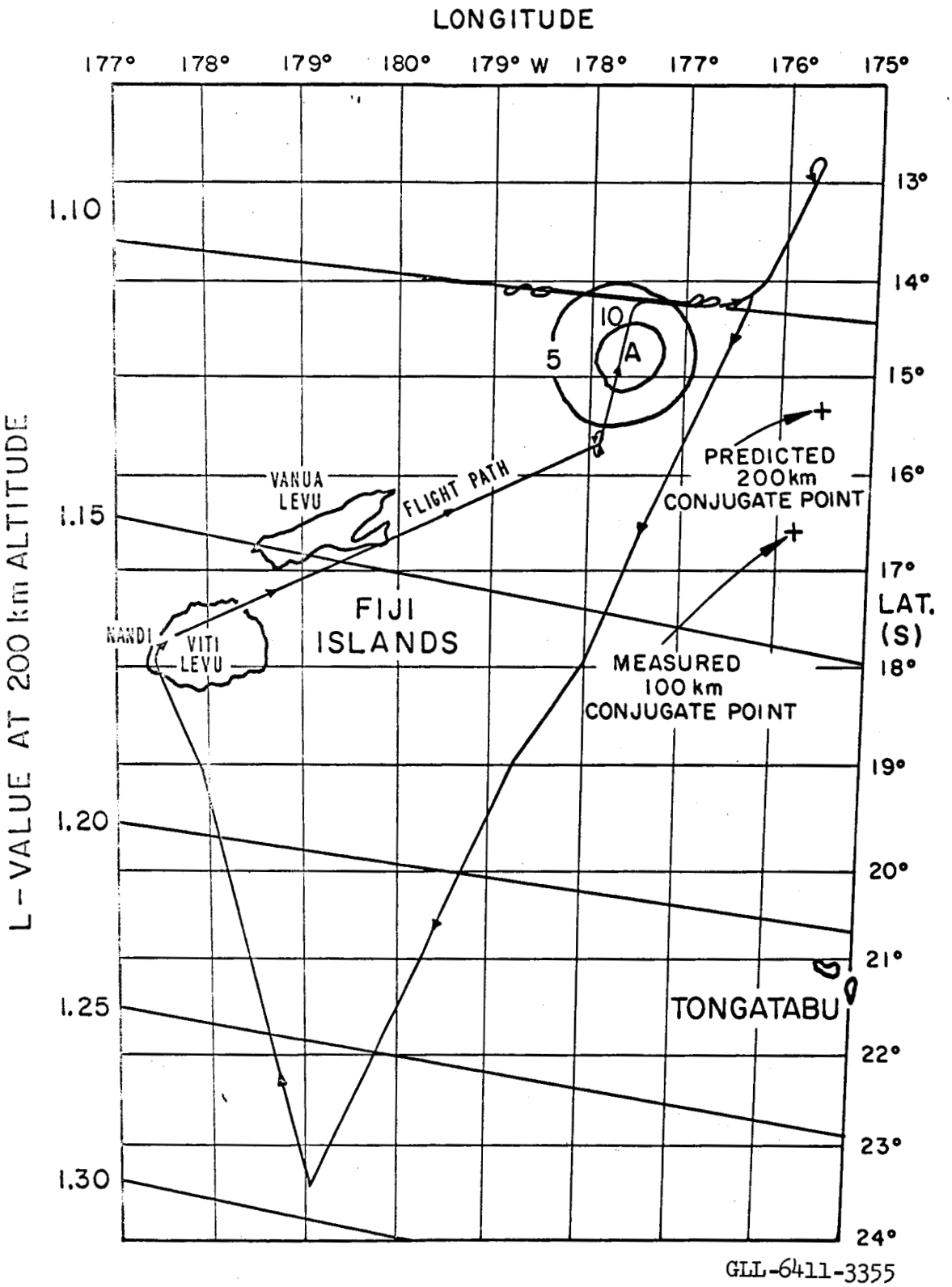

Fig. 12. Contour map of inferred debris distribution within 30 min of the detonation with 100 and 200 km conjugate points [Leonard, 1963] and with L-values of magnetic field lines at expected debris stopping altitude above aircraft (200 km)[Harrison et al., 1963].

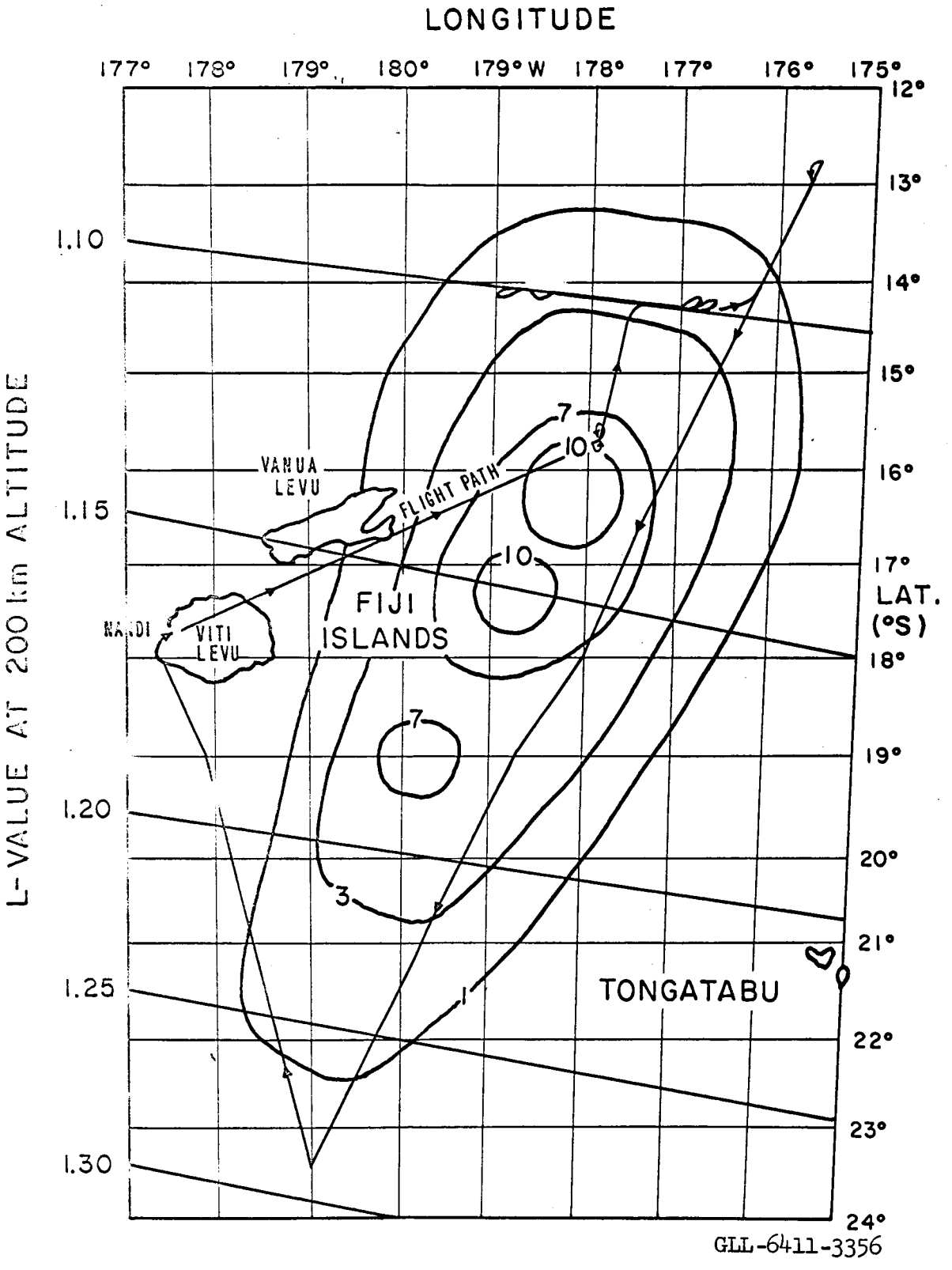

Fig. 13. Contour map of inferred debris distribution from 90 to 210 min after the detonation, with L-values of magnetic field lines at expected debris stopping altitude above aircraft (200 km) [Harrison et al., 1963].

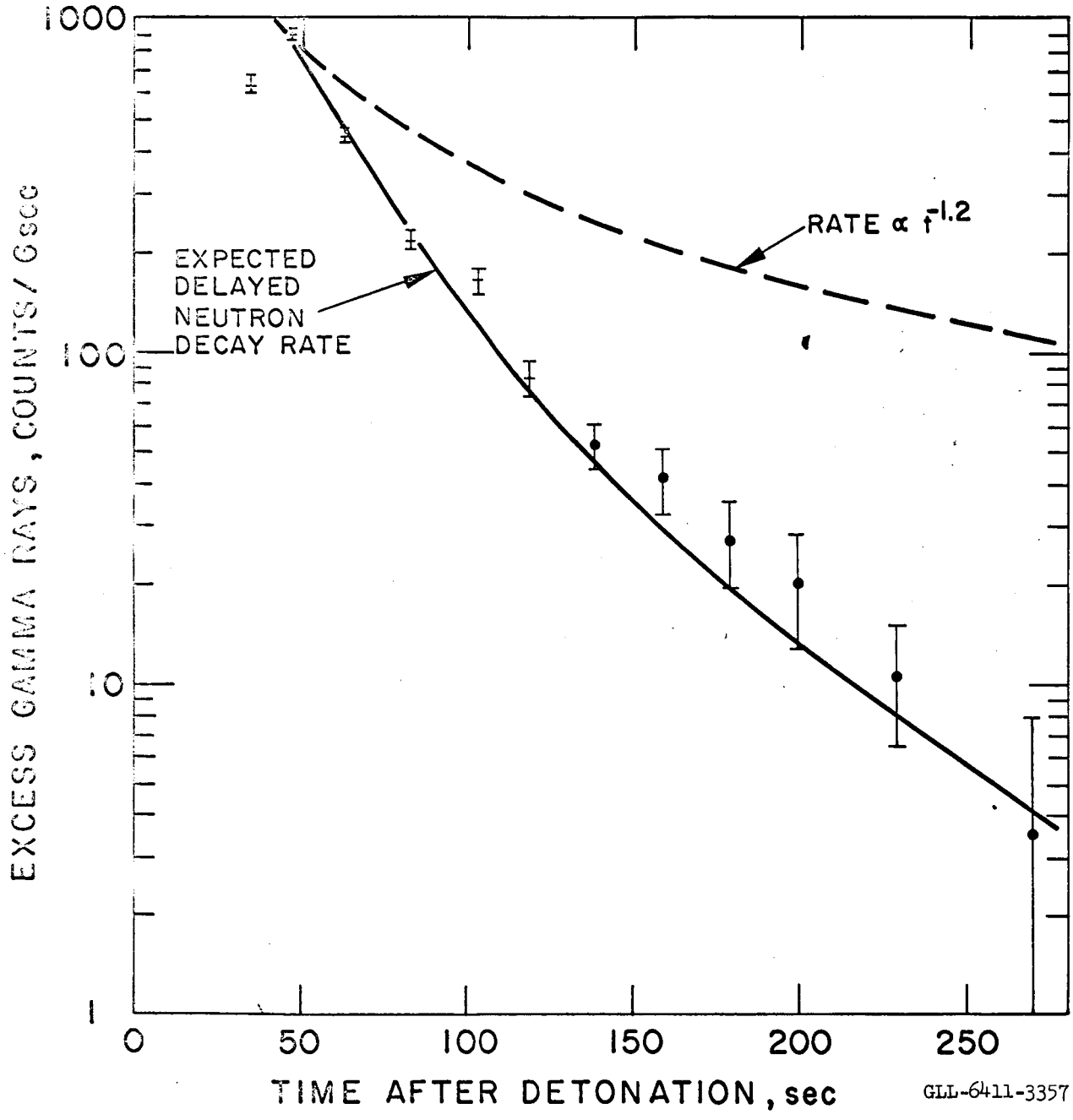

Fig. 14. Time decay of 9- to 13-Mev gamma rays from 50 to 300 sec after detonation, with L-values of magnetic field lines at expected debris stopping altitude above aircraft (200 km) [Harrison et al., 1963].